Neurospine 2020;17(1):294-303.
https://doi.org/10.14245/ns.1938102.051

Neurospine
pISSN 2586-6583 eISSN 2586-6591

Original Article

Corresponding Author
Niladri Kumar Mahato
https://orcid.org/0000-0001-5439-1172

Department of Preclinical Sciences, Faculty of Medical Sciences, The University of The West Indies, St. Augustine Campus, Trinidad and Tobago
E-mail: nm620511@ohio.edu

Received: March 25, 2019
Revised: June 17, 2019
Accepted: June 17, 2019

Re-examining the Spectrum of Lumbosacral Transitional Dysmorphisms: Quantifying Joint Asymmetries and Evaluating the Anatomy of Screw Fixation Corridors

Niladri Kumar Mahato

Department of Preclinical Sciences, Faculty of Medical Sciences, The University of The West Indies, St. Augustine Campus, St. Augustine, Trinidad and Tobago

Objective: Although a wide range of sacral dysmorphisms has been documented with lumbosacral transitional vertebrae (LSTV) variations, quantitative characterization of the upper segment morphology and articular anatomy across the array of lumbosacral transitions are hardly found in the literature. This study presents LSTV anomalies as a series of sequential morphological changes (the LSTV spectrum) and quantitatively compares 6 LSTV subtypes with normative sacral dimensions including the anatomy at the upper sacral segments used for percutaneous sacroiliac screw insertion.
Methods: Seven linear dimensions were measured from LSTV subtypes and normal sacral variants from dried adult sacral specimens. The auricular, superior articular and facet surface areas were quantified. Obliquity and thickness of osseous corridors used for sacroiliac screw fixation were measured. Data were statistically compared within and between LSTV subtypes and the normal variants.
Results: LSTVs presented a wide range of morphometric differences in comparison to the normal bones. Grouping LSTV according to auricular surface positions (high, normal, and low) demonstrated significant between-group differences in the obliquity and thickness at the S1 and S2 segmental corridors.
Conclusion: Frequent occurrence of LSTV in the general population may require evaluation of anatomical parameters in these variations for safe sacroiliac instrumentation around this region.

Keywords: Auricular surface, Lumbarization, Osseous corridors, Sacralization, Sacroiliac, Lumbosacral transitional vertebrae

INTRODUCTION

Identification of lumbosacral transitional vertebrae (LSTV) is essential for accurate determination of the number of thoracolumbar vertebrae. Such numerical identification is required to ascertain visceral position corresponding to a specific vertebral level.[1-5] However, the biomechanical importance LSTV-related alterations at the sacroiliac articular symmetry, facet dimensions, and associated lumbosacral anatomy have been relatively underreported.[6-9] The 2 classification systems currently available to characterize LSTV focus only at the lumbosacral junction.[10,11] Consequently, these classification systems do not recognize associated morphological alterations that accompany LSTV variations including the change in the number of sacral segments and lumbar vertebrae, asymmetries of load-bearing surfaces and facet dimensions, and overall sacral anatomy that result from

Table 1. Castellvi lumbosacral transitional vertebrae (LSTV) classification

LSTV type†	Subtype	Anatomical criteria	Prevalence
Type I	Unilateral (Ia)	Transverse process(es)‡ ≥ 19 mm (craniocaudal dimension)	~40%
	Bilateral (Ib)		
Type II	Unilateral (IIa)	Di-arthrodial joint: transverse process(es) with the sacral ala/e	-
	Bilateral (IIb)		
Type III	Unilateral (IIIa)	Complete osseous fusion: transverse process(es) to the sacral ala/e	~11.5%
	Bilateral (IIIb)		
Type IV	-	Unilateral type II transition with a contralateral type III	~5.25%

The overall LSTV prevalence of ranges between 4.0% to 35.9%.[10]
†Castellvi classification does not distinguish lumbarization (separation of the upper sacral segment) and sacralization (addition of L5 as the upper sacral segment) of the lumbar spine while considering the lumbosacral junction. The biomechanical implications of the disparity in the number of sacral segments in these 2 conditions thus get overlooked in this classification. ‡Craniocaudal dimension of the transverse process at the lumbosacral junction. Castellvi classification does not specify if the transverse processes belong to an L5 vertebra (L5–S1 accessory articulation), L4 vertebra (in sacralization), or L6 vertebra (in lumbarization).[12]

inclusion or exclusion of vertebral segments into the sacral mass.[12]

The Castellvi transitional lumbosacral classification categorizes LSTVs as 4 types (I to IV) (Table 1). This classification system does not (1) segregate lumbarization (4-segment sacrum) from sacralization (6-segment sacrum) as 2 distinct anatomical entities, and interchangeably uses the terms sacralization and lumbarization; (2) point out common asymmetries seen with LSTV, nor (3) indicate any potential facet or pedicular anomalies associated with such transitions that may point out potential anomaly in load-bearing at the sacro-iliac joint (SIJ) or the facet joints.[10] LSTV reports starting with Bertolotti in 1917 have attempted to explore the etiological relationship between transition-specific morphology and back pain.[11,13] None of the LSTV classification systems or morphological reports discuss specific LSTV-induced changes at the upper sacral segments and osseous corridors in the context of sacroiliac implant insertions.

The prevalence of LSTV is estimated at 12.5% (range, 4.0%–35.9%).[9,14] With the increasing evidence of biomechanical anomalies, the incidence of low back pain and sacroiliac dysfunctions in LSTV, anatomical studies about surgical access at LSTV-associated lumbosacral and sacroiliac regions become important.[1,15-21] Accordingly, this study has attempted to (1) elucidate LSTV as a series of morphological changes (the LSTV spectrum) involving sequential exclusion or inclusion of additional vertebral segments into the sacrum; (2) quantify sacral dimensions across this transitional spectrum, comparing parameters within and between LSTV subtypes and normal variants, and (3) quantify sacroiliac screw-placement corridors in LSTV subtypes and the normal variants from a large cohort of sacral specimens.

MATERIALS AND METHODS

1. Sample Selection

Dried human sacra used in this study were obtained from cataloged osteological repositories of medical schools across central, western and southern provinces in India. The bones selected for measurements (n = 220) were completely ossified, belonged to adults of both genders, and were screened for damage or breakage. These randomly selected samples were then screened for features of lumbosacral transitions (n = 63).

2. LSTV Spectrum

Selected samples were arranged in a series of groups representing subsets of lumbosacral transitions starting with the 4-segmented sacrum (lumbarization), next including the normal 5-segmented sacrum, and ending with the 6-segmented (sacralization) samples on the other side of this LSTV spectrum. Samples with accessory lumbosacral (L5–S1/L6–S1) articulations and those with incomplete fusions were placed at corresponding positions (depending on their number of sacral segments) within this LSTV spectrum (Figs. 1, 2). The *lumbarized wing* of the spectrum (Fig. 1) comprised (1) complete lumbarization (CL); (2) CL with unilateral or bilateral L6–S1 accessory articulation (AA) between the transverse process (TP) and sacral ala; (3) Incomplete lumbarization (IL), 5-segment sacrum presenting unilateral separation between S1–2 transverse elements, with or without separation at the S1–2 bodies; (4) Normal sacrum (N) with 5 segments, at the *center* of the LSTV spectrum. The *sacralization wing* (Fig. 2) included (5) unilateral or bilateral enlargement of L5 TP forming L5–S1 AA in a 5-seg-

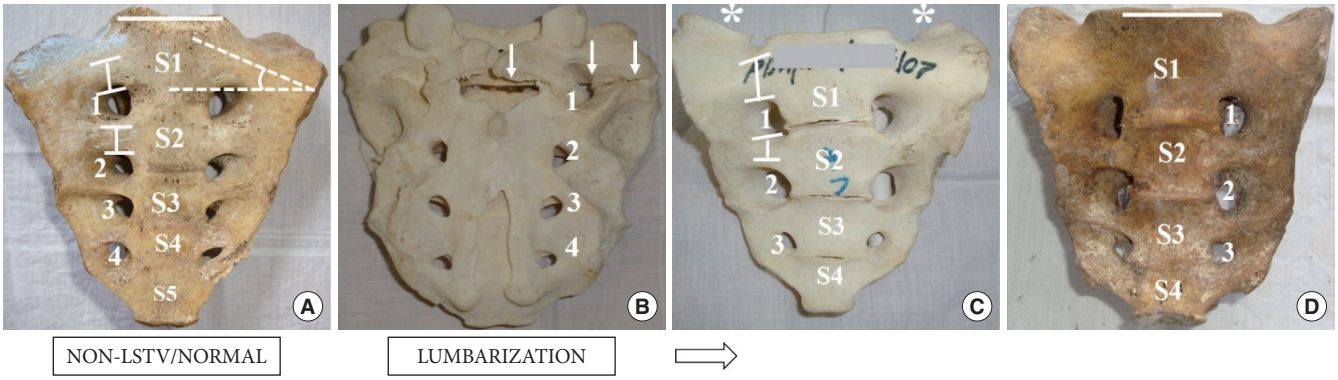

Fig. 1. Lumbosacral transitional vertebrae spectrum (LSTV) (lumbarization). The panel diagram (A-D) depicts the progression of lumbarization as a series of anatomical changes. The arrow shows the direction of decrease in the number of sacral segments from 5 to 4. (A) Five-segment sacrum (S1–5), anterior foramina (1–4), the capped vertical bars on the transverse processes of the upper 2 sacral segments represents the thickness of the osseous corridors (S1T and S2T), the angle denoted by the dashed lines represent the measured obliquity of the first segment (S_1O), the horizontal bar over the first sacral segment is given to compare the plane of the S1 superior articular surface and the cranial level of the sacral ala. (B) Dorsal sacral foramina (1–4), the downward arrows show a partial separation of the S1 from the rest of the sacrum. (C) A 4-segment sacrum presenting bilateral accessory articulation (*). (D) Complete lumbarization, 4-segment sacrum.

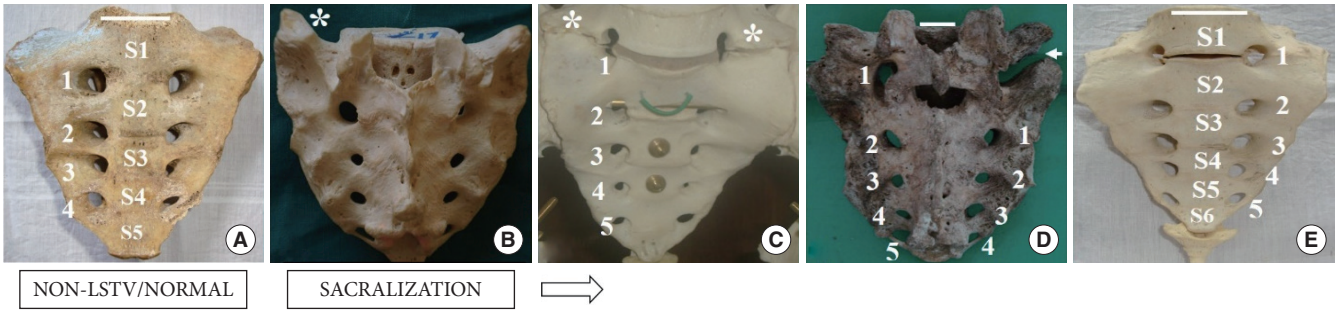

Fig. 2. Lumbosacral transitional vertebrae spectrum (LSTV) (sacralization). The panel diagram (A-E) depicts the serial progression to sacralization. The arrow shows the direction of an increase in the number of sacral segments from 5 to 6. (A) Five-segment sacrum (S1–5) sacrum, anterior sacral foramina (1–4). (B) Five-segment sacrum showing L5–S1 accessory articulation (*). (C) Bilateral L5–S1 accessory articulation (*). (D) Incomplete sacralization showing unfused right side (arrow). (E) Complete sacralization with 6 segments (S1–6) and anterior foramina (1–4). Horizontal bars on top of the first sacral segments represent the plane of the S1 superior articular surface. Note the accentuated alar slope with sacralization.

ment sacrum; (6) incomplete sacralization (IS), one-sided L5–S1 fusion on a 5-segmented sacrum; and (7) complete sacralization (CS) with bilaterally fused L5–S1 segments resulting in a 6-segment sacrum (Figs 1, 2; Table 2).

3. Anatomical Measurements

1) Linear dimensions

(1) sacral height (SH) in the midline, measured from the midpoint of the sacral promontory to the base of the sacrum. SH is the maximum sagittal dimension of the sacrum; (2) auricular surface height (AH): from the midpoint of the upper margin of the auricular surface (AS) to the lower extent of the AS. The upper point of AH corresponded to the thickest part within the lateral S1 alar mass in the coronal plane. (3) Inter facet distance (IFD): between the dorsal edges of the 2 facet joints; (4) inter auricular distance (IAD): between the midpoints of the superior margins of the 2 articular surfaces. IAD represented the maximum transverse dimension of the sacrum; (5) alar width (AW): the calculated difference between IAD and the S1 body width (BW). AW represented the maximum transverse thickness of the S1/upper osseous corridor. (6) BW: the maximum coronal distance on top of the first sacral segment. Measured as the transverse distance between midpoints of the upper 2 ventral sacral foramina; (7) facet depth: the perpendic-

 https://doi.org/10.14245/ns.1938102.051

Table 2. The lumbosacral transitional vertebrae (LSTV) spectrum and subtype distribution found in this study

Type	◄----- LSTV spectrum -----►						
	Complete sacralization (CS)	Incomplete sacralization (IS)	Accessory articulation (AA)	Normal (N)	Incomplete lumbarization (IL)	Accessory articulation (AA)	Complete lumbarization (CL)
Total (n = 220)	13/220 (8.63)	8/220 (3.64)	17/220 (9.54)	157/220 (66.81)	5/220 (2.27)	9/220 (3.18)	11/220 (5.9)
Type I/normal	3/13 (23.07)	-	2/17 (11.76)	103/157 (65.6)	-	2/9 (22.2)	1/11 (9.09)
Type II/high	-/13	-	11/17 (64.70)	35/157 (22.29)	-	7/9 (77.7)	9/11 (81.8)
Type III/low	10/13 (76.92)	-	-/17	19/157 (12.10)	-	-/9	2/11 (18.1)

Values are presented as number (%).
Arrows denote the direction of increase (left) or decrease (right) in the number of sacral segments between CL and CS LSTV spectrum including the normal 5-segment sacrum.

ular sagittal distance from the coronal plane of the IFD to the dorsal edge of the first sacral segment (Fig. 3A; Tables 3, 4).

2) Surface areas

(1) the right and left auricular surface areas (ASA); (2) the right and left facet surface areas (FSA); and (3) the body surface area. Unpaired Student t-test was applied to test the significance of differences for each parameter within and between-subtypes, including the normal sacrum, across the LSTV spectrum (Table 3).

3) Transverse element obliquity (S_1O)

The obliquity of the transverse elements (alar slopes) of the upper segments was measured bilaterally as S1 obliquity (S_1O) in the coronal plane. The distance between the midpoint of the sacral promontory and the AS was measured along the axis of the S1 transverse element. The superior border of the segment below was taken as the horizontal reference line. The angles were measured at the point close to the AS where the upper segmental line and the horizontal reference lines intersected. All angles were measured in the coronal plane using a protractor and averaged for both sides in the case of symmetric LSTVs (Table 4).

4) Transverse element thickness

The craniocaudal thickness of the transverse elements of the first (S1 thickness [S_1T]) and second (S2 thickness [S_2T]) sacral transverse elements or S1 and S2 osseous corridors were measured longitudinally between the midpoints of the corresponding ventral foramina across the segments (Table 4).

4. Types of AS Position

All samples were arranged into 3 groups as per the position of the AS relative to the lateral sacral mass.[22] An imaginary transverse plane joining the cranial end of the AS was used as reference to determine the relative position of the sacral AS. (1) Type I/normal: the transverse plane passing through the upper half of the S1segment (i.e., above the midpoint between sacral promontory and the lower border of the S1 body); (2) type II/high: the transverse plane passed above the sacral promontory, and (3) type III/low: the transverse plane passed below the midpoint between the sacral promontory and the lower border of the S1 body, or lower. S1 alar slopes were noted for any acute changes

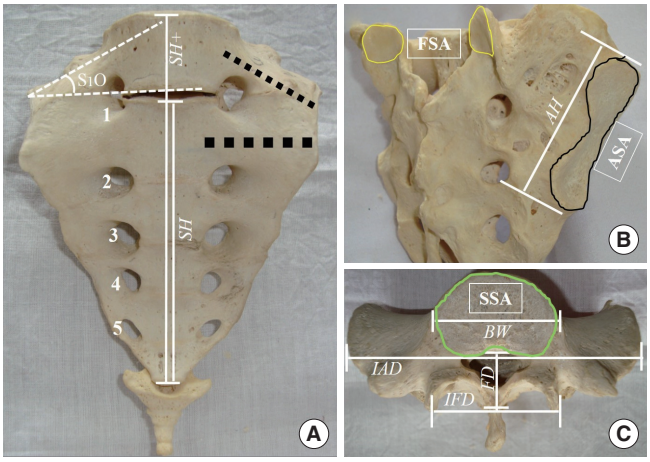

Fig. 3. Dimensions measured in the sacral specimens. Linear dimensions (italicized): sacral height (SH), auricular height (AH), inter facet distance (IFD), inter auricular distance (IAD), S1 body width (BW), and facet depth (FD). (A) Sacralized (6-segment) specimen, SH and the SH+ represent sacral heights in normal (5-segment) and sacralized (6-segment) examples, respectively. Anterior foramina are numbered 1–4, note the accentuated obliquity of the first segment (S_1O), grey thick dotted lines represent the potential trajectory of sacral screw placement through the upper 2 sacral corridors. Surface areas (bold, boxed): (B) Auricular surface area (ASA) outlined black, facet surface area (FSA) outlined white. (C) Superior surface area (SSA) outlined green.

Table 3. Linear dimensions and articular surface areas across the spectrum as per the number of segments fused into the sacrum (lumbarized to sacralized, from left to right)

Variable	Complete lumbarization (4 segments)	Incomplete lumbarization		Normal (5 segments)	Accessory articulation	Incomplete sacralization		Complete sacralization (6 segments)
Linear dimension (mm)								
Sacral height	90.78* ± 15.17	-	105.37 ± 15.32	105.05 ± 10.24	92.34 ± 9.39	-	102.14 ± 12.05	114.67 ± 12.4
Auricular surface height	59.55 ± 5.16	59.6† ± 4.03	61.7‡ ± 4.9	61.15 ± 8.16	59.53 ± 6.96	58.4† ± 3.04	63.09‡ ± 1.02	62.22 ± 4.3
Inter facet distance	47.35 ± 5.66	-	47.73 ± 11.45	52.12 ± 4.34	47.12 ± 5.84	-	45.13 ± 3.94	46.55 ± 4.34
Inter auricular distance	101.53 ± 9.02	-	94.02 ± 15.63	102.79 ± 10.09	100.22 ± 8.83	-	101.43 ± 6.21	98.24 ± 8.83
Alar width bilateral	60.98 ± 4.9	-	48.28* ± 11.93	56.45 ± 3.47	58.73 ± 0.87	-	55.04 ± 1.76	51.39 ± 2.84
S1 body width	40.55* ± 4.12	-	45.74 ± 3.7	46.34 ± 6.62	41.49 ± 7.96	-	46.39 ± 4.45	46.85 ± 5.99
Facet depth	13.25 ± 5.46	-	14.14 ± 2.35	15.24 ± 2.9	12.33 ± 2.79	-	14.33 ± 3.35	16.58 ± 2.76
Surface area (cm^2)								
Auricular surface area	9.75 ± 1.24	8.03†* ± 1.09	9.14‡ ± 1.19	10.36 ± 1.86	10.56 ± 2.33	8.53† ± 0.32	9.56‡ ± 0.68	9.82 ± 1.24
Superior surface area	8.35 ± 1.96	-	8.85 ± 1.23	10.02 ± 2.35	9.89 ± 3.32	-	9.46 ± 0.76	10.09 ± 3.32
Facet surface area	1.31 ± 0.56	1.85† ± 0.38	1.93‡ ± 0.26	1.71 ± 0.51	1.29* ± 0.42	1.43† ± 0.23	1.53‡ ± 0.11	1.47 ± 0.46

Values are presented as mean ± standard deviation.
Blank cells (-) denote variants that do not present a measurable anatomical feature on one side (incomplete fusions).
*Statistical significance detected with unpaired t-test ($p \leq 0.05$) comparing 2 groups in the lumbosacral transitional vertebrae spectrum representing the maximum and the minimum values for a given parameter. †Unfused side. ‡Fused side.

Table 4. Three types of auricular surface positions

Variable	Type II/ high	Type I/ normal	Type III/ low
Linear dimension (mm)			
Sacral height	94.82* ± 7.81	105.05 ± 10.24	108.4 ± 14.72
Auricular surface height	60.04 ± 6.36	61.15 ± 8.16	61.97 ± 5.01
Inter facet distance	102.04 ± 6.3	102.79 ± 10.09	100.86 ± 10.25
Inter auricular distance	42.9 ± 5.9	46.34 ± 6.62	46.97 ± 5.63
Alar width bilateral	47.88 ± 5.07	52.12 ± 4.34	47.9 ± 6.1
S1 body width	59.14 ± 3.4	56.45 ± 3.47	53.89 ± 4.62
Facet depth	13.98 ± 2.7	15.24 ± 2.9	15.88 ± 3.62
Surface area (cm^2)			
Auricular surface area	10.98 ± 1.78	10.36 ± 1.86	10.06 ± 1.58
Superior surface area	9.85 ± 2.3	10.02 ± 2.35	9.89 ± 2.82
Facet surface area	1.52 ± 0.48	1.71 ± 0.51	1.77 ± 0.48
Transverse element obliquity & thickness			
S1 obliquity of the upper osseous corridor (°)	16.64 ± 2.40	25.30 ± 3.79	30.6* ± 5.82 33.0* ± 4.33
S1 craniocaudal thickness (mm)	21.90 ± 3.41	19.40 ± 4.88	21.10 ± 2.39 13.88* ± 3.45
S2 craniocaudal thickness (mm)	14.56 ± 3.14	13.60 ± 2.45	15.64 ± 2.67 19.48* ± 3.40

*Statistical significance detected with unpaired t-test ($p \leq 0.05$) comparing 2 groups in the lumbosacral transitional vertebrae spectrum with the maximum and the minimum values for a given parameter. Italicized and bold values in C represents sacralization samples, only.

in sacroiliac sagittal angulations, and for variations in the shape of the first anterior sacral foramina in the LSTV samples. Linear dimensions were measured by a digital sliding caliper (sensitivity, 0.01 mm) (Global Industrial, Port Washington, NY, USA). All surface areas were circumscribed on a tracing paper placed snugly over the articular surfaces. The circumscribed articular surface areas were measured by a digital planimeter. Statistical calculations had been performed using the SPSS ver. 17.0 (SPSS Inc., Chicago, IL, USA) software (Fig. 4, Table 4).

RESULTS

This study detected 28.6% (63 of 220) samples with LSTV variations, including all its subtypes (Table 2). Within-subtype LSTV samples did not present any statistically significant differences in the measured dimensions. As a result, data were pooled within each LSTV subtype for comparison with the normal variants. As described below, several parameters demonstrated statistically significant differences when compared across the LSTV spectrum (Table 3). No within or between-subtype, or male to female comparisons were performed due to the unequal distribution of gender-specific samples in each subtype, and due to a very few male samples available on the lumbarization end of the spectrum and vice-versa.[23]

https://doi.org/10.14245/ns.1938102.051

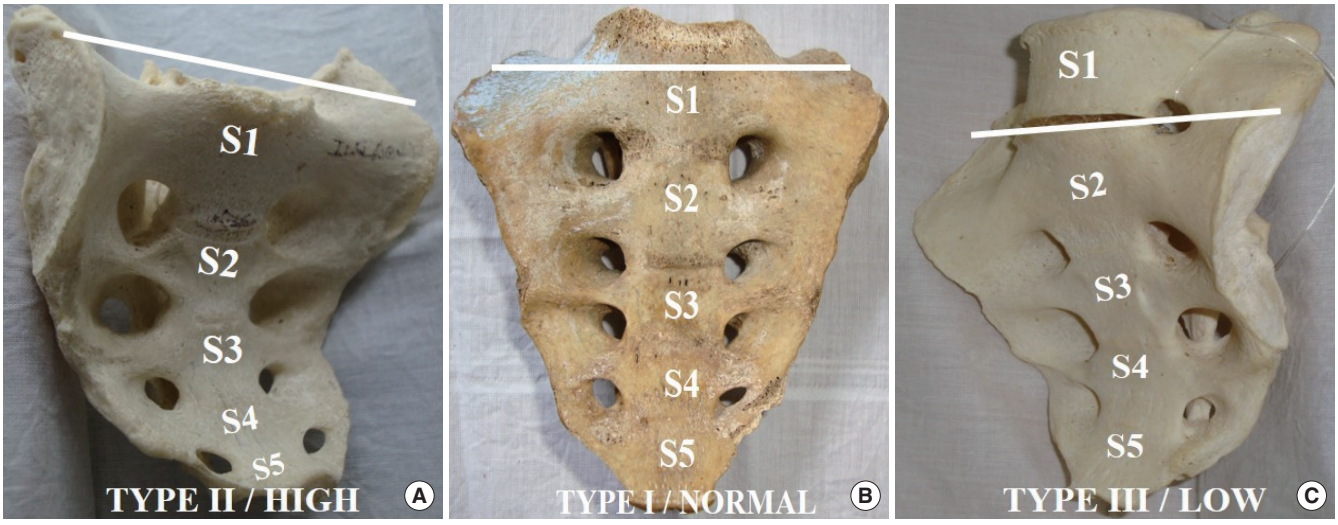

Fig. 4. Auricular surface positions. The panel diagram shows the 3 different types of auricular surface (AS) positions in 5-segment sacra. The horizontal bars represent the upper limits of the AS for comparing it with the top of the S1 sacral segment. Changing positions of the AS correspondingly alter the obliquity of the transverse sacral elements even in a normal 5-segment sacrum, moving from left to right in this figure.

1. Linear Dimensions and Surface Areas (Table 3)

Among the 8 LSTV subtypes identified in this study, linear dimensions and surface area data from the CL and CL with AAs were pooled together. Most CLs presented with unilateral or bilateral AAs. Linear dimensions in both the variants did not demonstrate any statistically significant difference. AH values from IL and IC have been presented and compared between the unfused and fused sides.

Data from surface areas ASA and FSA of the 2 sides were pooled together as no significant side-specific differences could be detected using the t-test. ASA from the IL and IC have been presented and compared separately with the unfused and fused sides. Several facets in the AA variety presented tropisms and in some instances were observed to be uni- or bilaterally rudimentary and with coronal orientations.[24,25]

Some important changes observed across the LSTV subtypes across the spectrum from CL to CS: (1) although the SH gradually increased with addition of extra sacral segments, only 2 of the linear dimensions (AW and BW) and 1 surface area (ASA) presented statistically significant between-subtype changes. Accordingly, loading asymmetries may be critical for sacroiliac pain instead of the absolute magnitude of loading, as indicated by comparatively less variability in the overall sacral size even with LSTV.

2. Linear Dimensions and Surface Areas as per AS Position

Linear dimensions and surface areas as seen with the samples arranged according to 3 different AS positions, the only demonstrated a significantly smaller SH in type II/high AS samples (Fig. 4, Table 3).

3. Obliquity of the Upper Transverse Element in LSTV Subtypes

Type I/normal AS, type II/high AS, and type III/low AS showed differences in S1 osseous corridor obliquity in the coronal plane. Additionally, CL (6-segment sacrum) and partially lumbarized (separated at the S2–2 bodies) angles showed significantly accentuated obliquity than the normal and other LSTV subtypes (Table 4).

4. Thickness of the Transverse Element in LSTV Subtypes

Type I/normal AS, 5-segment sacrum demonstrated greater thickness at the upper (S1) transverse elements as compared to CL (4-segment) specimen. The S2 thicknesses differed between LSTV subtypes, with the S_2T in CS specimen demonstrating a 'reversal' of S1–2 thickness pattern. In CS, the S2 transverse element thickness significantly increased in contrast to S1, both in the between-group and within-group comparisons (Fig. 3, Table 4).

DISCUSSION

Several studies have reported the anatomy of osseous screw insertion corridors across the upper sacral segments.[19-21,26-33] Al-

most all of these studies have described percutaneous screw insertion segments in the context of normal, 5-segment sacra. It is rare to find reports that discuss the screw insertion anatomy in the context of the variability of sacral morphology seen in transitional lumbosacral variations.[1,34,35] LSTV anatomy in the setting of sacroiliac joint instrumentations can hardly be overemphasized given the variations presented in the sacral anatomy and the vicinity of vital neurovascular structures along the trajectory of screw placement through the upper osseous corridors in the sacrum. This study presents a detailed report on quantitative assessment of LSTV-related sacral anatomy and, at the same time, identifies and compares differences in dimensions between the normal sacrum and those that are associated with lumbosacral transitional subtypes in context of sacroiliac screw insertion. Descriptive data on linear dimensions, articulating surface areas, segmental thickness, and obliquity have been reported in this study. Some of the more specific observations about percutaneous sacroiliac screw insertion have been discussed below.

This study, for the first time, reports the significant differences in sacral auricular height, articular surface area asymmetries, upper sacral segment anatomy observed between different LSTV subtypes and normal variants. This study observed dysmorphisms involving enlarged sacral mamillary processes (MP) present in all sacrum except ones with high (type II) ASs. Both IL/CL and IS/CS presented large MPs but not sacrum presenting accessory lumbosacral articulations. S1 MPs observed in high (type II) ASs demonstrated near-complete absorption or assimilation of the MPs that appeared smaller and rudimentary. This may be the reason for the S1 transverse element (S_1T) being thicker in sacrum with high up AS (Table 4).

1. Altered Obliquity and Thickness of the First Sacral Segment

1) Five-segment sacrum and type I/normal AS

The average obliquity (S_1O) of the upper sacral (S1) corridor with the normal position of the AS or a 5-segment sacrum was 25.30° ± 3.79°. The first sacral osseous corridor thickness (S_1T) was found to be 19.40 ± 4.88 mm and was greater than the second corridor (S_2T) measuring 13.60 ± 2.45 mm.

2) Lumbarization and type II/high AS

Such variations presented a lesser average obliquity (S_1O) of the upper sacral (S1) corridor 16.64° ± 2.40° compared to (a). However, the first sacral osseous corridor thickness (S_1T) measured 21.90 ± 3.41 mm and the second corridor (S_2T) 13.60 ± 2.45 mm.

The first and second sacral corridors in (b) measured slightly greater than in (a) possibly due to greater absorption of the MPs into the sacral segments.

3) Type III/low AS

In general, all sacrum presenting low positions of the AS significantly increased the S_1O, measuring 30.6° ± 5.82° on an average. Such an increase in the superior corridor obliquity slightly reduced its thickness of 21.10 ± 2.39 mm, in comparison to (b). On the other hand, the second corridor thickness was seen to be increased by 15.64 ± 2.67 mm, in comparison to the other groups.

4) Sacralization

Though sacrum with sacralization presented similar patterns of alterations as seen with type II/low AS (c), this group presented the most significant absolute changes in parameters measured across the LSTV spectrum. In addition to the lower AS position, sacralization presented significant accentuated S_1O 33.0° ± 4.33°. The S_1T demonstrated a significant reduction 13.88 ± 3.45 mm, whereas the S_2T showed significant thickening 19.48 ± 3.40 mm. Thus, with sacralization, not only the AS shifts to a lower position, the obliquely of the upper corridor is accentuated, and the S2 corridor assumes a more transverse position. Similar features are seen with IS or lumbarization, on the ipsilateral side of the unilateral LSTV variation. Thus, instrumentation in bi-, unilateral sacralization, and in sacrum with type II/low AS may need careful assessment of the increased obliquity and reduced girth of the S1 transverse element. Therefore, the sacralization LSTV subtype may denote a 'reversal' in the roles of S1 and S2 corridors in terms of osseous screw anchorage given the change in their dimensions. Since in sacralization, the L5 TP forms the cranial osseous corridor, it is relatively thinner. In contrast, the original upper sacral segment (now representing the S2 corridor) remains enlarged and forms the main osseous corridor for a sacroiliac screw placement. With increasing obliquity of the S1/upper transverse element, the transverse S2 corridors, assume a higher transverse plane closer to the upper end of the iliac articular surface.

This study reports that with sacralization, or enlargement of the S1 MP accentuates the concavity anterior to the S1 ala by reducing the alar mass ventrally. Exteriorization of the implant in this region may be a concern (Fig. 5). The upper sacral segments in some sacra may be found tilted dorsally that brings the S1 osseous corridor to a more posterior plane and increases

 https://doi.org/10.14245/ns.1938102.051

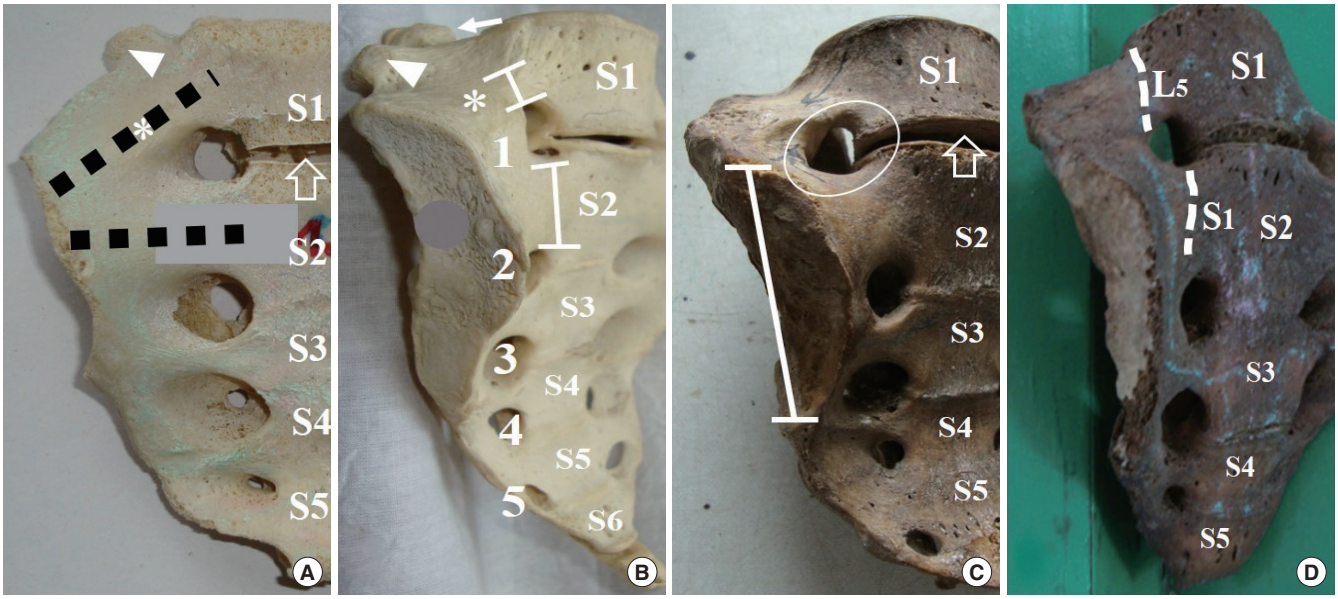

Fig. 5. Lumbosacral transitional vertebrae spectrum: some important considerations in sacroiliac screw fixation. (A) Five-segment sacrum (type III/low auricular surface [AS]) with wide S1–2 disc space (open arrow), shows acutely sloping ala (*), enlarged S1 mamillary process (arrowhead), trajectory of screw placement illustrated with black dashed lines through the first and second segment corridors. (B) Complete sacralization showing sloping ala (*). Note that sacralization increases the obliquity of the S1 corridor, it significantly reduces the S1 corridor thickness compared to the more transverse S2 corridor (capped vertical bars). Anterior foramina (1–5), segments (S1–5), the L5 mamillary process (arrowhead), and the ipsilateral facet joint (arrow). (C) Complete sacralization with wide S1–2 disc space (open arrow), Type III/low AS as in panel B (capped vertical bar), and a dysmorphic first anterior foramen (encircled). (D) Five-segment sacrum with a dorsally tipped S1 segment and loss of ventral concavity. Dorsal tilting of the S1 ala brings the corresponding L5 ventral rami (upper dashed line) closer to the sacral ala. Note the type III/low AS associated with this variant.

vulnerability of the nerve-root to instrumental injury. Wider disc spaces at the upper segments representing partially fused discs can be seen in CS, CL, and partial fusions. Normal, AA rarely present this feature. This study has reported the presence of irregular anterior sacral foramen with LSTV (sacralization) but not with other types of LSTV. The tongue-in-groove interosseous interdigitations featuring in the retro-articular part of SIJ articulations are constant features of normal and dysmorphic LSTV variations.[6,29,31,34] As observed in this study, identifying the type of AS position may be a good indicator to assess the obliquity and of the upper 2 sacral segments. It will be worth mentioning here that individual 3-dimensional reconstruction of lumbosacral computed tomography (CT) gives accurate case-based anatomical information in patients. However, this study has highlighted that a lumbosacral CT scan may not provide the exact number of lumbar vertebrae found with LSTV lumbar vertebral anomalies. This study provides the anatomical details of different sacral components such as AS, facet, and superior articular area variations in the context of specific LSTV subtypes. Dimensions reported from a large cohort of LSTV samples in this study may provide a database for clinicians and researchers to look for specific associations between sacral variabilities in LSTV subtypes. Additionally, this study has compared the anatomy of the LSTV spectrum with the normal variants that may be used to understand the biomechanical implications of load-bearing across the lumbosacral and sacroiliac articulations. Also, the study has attempted to present the array of LSTV variations as a spectrum of changes occurring in the sacral anatomy across LSTV subtypes as a series of evolving biomechanically related adaptive alterations.

CONCLUSION

Transitional lumbosacral changes present a range of structural alterations in the segment number, size, area, and position of the articular surfaces and the alar slope, in the sacrum. LSTV sacral anatomy may present challenges for instrumentation at the sacroiliac region. Recognition of such variabilities is a prerequisite for safe and successful SIJ instrumentation in such a scenario.

CONFLICT OF INTEREST

The authors have nothing to disclose.

REFERENCES

1. Josiah DT, Boo S, Tarabishy A, et al. Anatomical differences in patients with lumbosacral transitional vertebrae and implications for minimally invasive spine surgery. J Neurosurg Spine 2017;26:137-43.
2. Kassir MA, Al-Faham Z, Abel N, et al. Lumbosacral transitional vertebra diagnosed on 99mTc-methylene diphosphonate SPECT/CT. J Nucl Med Technol 2015;43:137-8.
3. Porter NA, Lalam RK, Tins BJ, et al. Prevalence of extraforaminal nerve root compression below lumbosacral transitional vertebrae. Skeletal Radiol 2014;43:55-60.
4. Hanson EH, Mishra RK, Chang DS, et al. Sagittal whole-spine magnetic resonance imaging in 750 consecutive outpatients: accurate determination of the number of lumbar vertebral bodies. J Neurosurg Spine 2010;12:47-55.
5. Delport EG, Cucuzzella TR, Kim N, et al. Lumbosacral transitional vertebrae: incidence in a consecutive patient series. Pain Physician 2006;9:53-6.
6. Postacchini R, Trasimeni G, Ripani F, et al. Morphometric anatomical and CT study of the human adult sacroiliac region. Surg Radiol Anat 2017;39:85-94.
7. Dar G, Peleg S, Masharawi Y, et al. Sacroiliac joint bridging: demographical and anatomical aspects. Spine (Phila Pa 1976) 2005;30:E429-32.
8. Mahato NK. Implications of structural variations in the human sacrum: why is an anatomical classification crucial? Surg Radiol Anat 2016;38:947-54.
9. Jancuska JM, Spivak JM, Bendo JA. A review of symptomatic lumbosacral transitional vertebrae: Bertolotti's Syndrome. Int J Spine Surg 2015;9:42.
10. Castellvi AE, Goldstein LA, Chan DP. Lumbosacral transitional vertebrae and their relationship with lumbar extradural defects. Spine (Phila Pa 1976) 1984;9:493-5.
11. O'Driscoll CM, Irwin A, Saifuddin A. Variations in morphology of the lumbosacral junction on sagittal MRI: correlation with plain radiography. Skeletal Radiol 1996;25:225-30.
12. Mahato NK. Redefining lumbosacral transitional vertebrae (LSTV) classification: integrating the full spectrum of morphological alterations in a biomechanical continuum. Med Hypotheses 2013;81:76-81.
13. Bertolotti M. Contributo alla conoscenze dei vizi di differenzazione regionale del racide con speciale riguardo alla assimilazione sacrale della V. lombare. Radiol Med 1917;4:113-44.
14. Konin GP, Walz DM. Lumbosacral transitional vertebrae: classification, imaging findings, and clinical relevance. AJNR Am J Neuroradiol 2010;31:1778-86.
15. Snijders CJ, Vleeming A, Stoeckart R. Transfer of lumbosacral load to iliac bones and legs Part 1: Biomechanics of self-bracing of the sacroiliac joints and its significance for treatment and exercise. Clin Biomech (Bristol, Avon) 1993;8:285-94.
16. Lingutla KK, Pollock R, Ahuja S. Sacroiliac joint fusion for low back pain: a systematic review and meta-analysis. Eur Spine J 2016;25:1924-31.
17. Paudel B, Kim HS, Jang JS, et al. Percutaneous full endoscopic treatment of bertolotti syndrome: a report of three cases with technical note. J Neurol Surg A Cent Eur Neurosurg 2017;78:566-71.
18. Goetzen M, Ortner VK, Lindtner RA, et al. Correction to: a simple approach for the preoperative assessment of sacral morphology for percutaneous SI screw fixation. Arch Orthop Trauma Surg 2018;138:889.
19. Gras F, Gottschling H, Schröder M, et al. Transsacral osseous corridor anatomy is more amenable to screw insertion in males: a biomorphometric analysis of 280 pelves. Clin Orthop Relat Res 2016;474:2304-11.
20. Goetzen M, Ortner K, Lindtner RA, et al. A simple approach for the preoperative assessment of sacral morphology for percutaneous SI screw fixation. Arch Orthop Trauma Surg 2016;136:1251-7.
21. Mendel T, Radetzki F, Wohlrab D, et al. CT-based 3-D visualisation of secure bone corridors and optimal trajectories for sacroiliac screws. Injury 2013;44:957-63.
22. Mahato NK. Variable positions of the sacral auricular surface: classification and importance. Neurosurg Focus 2010;28:E12.
23. Mahato NK. Relationship of sacral articular surfaces and gender with occurrence of lumbosacral transitional vertebrae. Spine J 2011;11:961-5.
24. Mahato NK. Association of rudimentary sacral zygapophyseal facets and accessory and ligamentous articulations: implications for load transmission at the L5-S1 junction. Clin Anat 2010;23:707-11.
25. Mahato NK. Facet dimensions, orientation, and symmetry at L5-S1 junction in lumbosacral transitional States. Spine (Phila Pa 1976) 2011;36:E569-73.
26. Conflitti JM, Graves ML, Chip Routt ML Jr. Radiographic quantification and analysis of dysmorphic upper sacral os-

https://doi.org/10.14245/ns.1938102.051

seous anatomy and associated iliosacral screw insertions. J Orthop Trauma 2010;24:630-6.
27. Eden SV. Surgical treatment for the painful, stable sacroiliac joint: what does the literature tell us? In: Dall BE, Eden SV, Rahl MD, editors. Surgery for the painful, dysfunctional sacroiliac joint: a clinical guide. Cham: Springer International Publishing; 2015. p. 7-14.
28. Esses SI, Botsford DJ, Huler RJ, et al. Surgical anatomy of the sacrum. A guide for rational screw fixation. Spine (Phila Pa 1976) 1991;16(6 Suppl):S283-8.
29. Miller AN, Routt ML Jr. Variations in sacral morphology and implications for iliosacral screw fixation. J Am Acad Orthop Surg 2012;20:8-16.
30. Miller LE, Block JE. Minimally invasive arthrodesis for chronic sacroiliac joint dysfunction using the SImmetry SI Joint Fusion system. Med Devices (Auckl) 2014;7:125-30.
31. Gardner MJ, Morshed S, Nork SE, et al. Quantification of the upper and second sacral segment safe zones in normal and dysmorphic sacra. J Orthop Trauma 2010;24:622-9.
32. Wu LP, Li YK, Li YM, et al. Variable morphology of the sacrum in a Chinese population. Clin Anat 2009;22:619-26.
33. Gras F, Hillmann S, Rausch S, et al. Biomorphometric analysis of ilio-sacro-iliacal corridors for an intra-osseous implant to fix posterior pelvic ring fractures. J Orthop Res 2015; 33:254-60.
34. Lee JJ, Rosenbaum SL, Martusiewicz A, et al. Transsacral screw safe zone size by sacral segmentation variations. J Orthop Res 2015;33:277-82.
35. Illeez OG, Atıcı A, Ulger EB, et al. The transitional vertebra and sacroiliac joint dysfunction association. Eur Spine J 2018; 27:187-93.